Ultrahigh-energy cosmic-ray signature in GRB221009A

Saikat Das

Yukawa Institute for Theoretical Physics, Kyoto University, Japan

Astrophysical Messengers

Electromagnetic Radiation:

Photons from luminous objects — 10^5 cm radio waves to 10^{-16} cm (∼ TeV) γ-rays

Cosmic Rays:

Protons and nuclei — ∼ MeV to ∼ZeV energies. Widely varying flux and composition

Astrophysical Neutrinos:

Photohadronic interactions – neutrinos and $\gamma-$rays. Weakly interacting & neutral.

Gravitational Waves:

Ripples in space-time – acceleration of massive objects – colliding compact objects

Cosmic background radiation

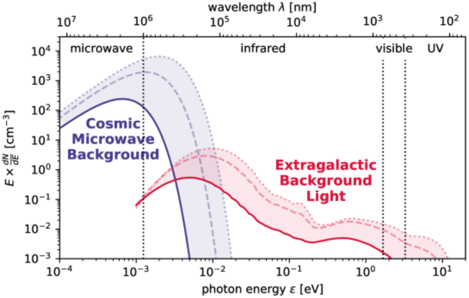

Figure: CMB & EBL spectrum at redshift 0 (solid), 1 (dashed), 2 (dotted). Image courtesy: Jonas Heinze (DESY)

CMB

- blackbody-radiation spectrum $T_0 \sim 2.7$ K
- originates from epoch of recombination
- does not receive additional injection
- scales purely adiabatically $T = (1+z)T_0$
- $n \sim 410$ cm^{-3}, energy $\bar{\epsilon}_{\rm bg} = 0.6$ meV

EBL

- cumulative redshifted radiation from stars
- constant injection following SFR
- re-emission by interstellar dust 2 peaks
- number density is ~1/200 that of CMB
- non-trivial redshift evolution

Cosmic Rays

- γ-rays from high-energy sources are produced by leptonic processes (synch, IC, etc.)
- The Universe is impenetrable to EM radiation at $\gtrsim$ TeV energies
- Cosmic Rays: – charged particles – primarily hadrons (atoms and nuclei)

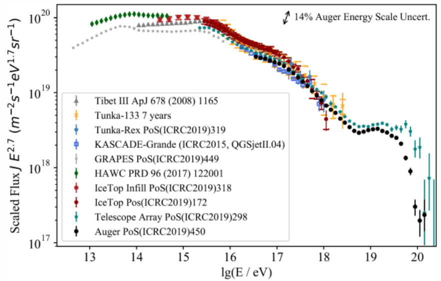

Figure: CR spectrum from ~TeV energies up to 100 EeV (Image: Frank G. Schröder, ICRC 2019, WI, USA)

knee $\approx 3 \times 10^{15}$ eV   ankle $\approx 5 \times 10^{18}$ eV   cutoff $\approx 4 \times 10^{19}$ eV

Ultra-high energy cosmic rays

1. Extragalactic astrophysical origin with energies > 10^{18} eV, produced in extreme explosions like AGNs, GRBs, BH accretion.
2. Interacts with cosmological photon backgrounds (CMB, EBL) and intervening magnetic fields.
3. Fermi acceleration: Energy gain through repeated reflection from magnetic mirrors. Unipolar induction: Relativistic magnetic rotators induce $E-$field.
4. Secondary particles are produced via numerous channels contributing to diffuse gamma ray and neutrino background.

Energy loss processes

Photopion production

$$p + \gamma_{\rm bg} \rightarrow \Delta^+ \rightarrow \begin{cases} p + \pi^0 \\ n + \pi^+ \end{cases}$$

$$\pi^+ \longrightarrow \mu^+ + \nu_\mu \rightarrow e^+ + \nu_e + \bar{\nu}_\mu + \nu_\mu$$

$$\pi^0 \longrightarrow \gamma + \gamma$$

Beta decay

$$n \longrightarrow p + e^- + \bar{\nu}_e$$

$$E_{\rm th}^{N,\pi} = \frac{m_\pi c^4 (m_N + m_\pi/2)}{2\epsilon}$$

$$\approx 6.8 \times 10^{19} A \left(\frac{\epsilon}{\rm meV}\right)^{-1} {\rm eV}$$

GZK phenomenon – flux suppression at $E > 4 \times 10^{19}$ eV

Pair-production

$${}^A_Z X + \gamma_{\rm bg} \rightarrow {}^A_Z X + {\rm e}^+ + {\rm e}^-$$

$$E_{\rm th}^{\rm e^\pm} = 4.8 \times 10^{17} A \left(\frac{\epsilon}{\rm meV}\right)^{-1} {\rm eV}$$

Photodisintegration

$${}^A_Z X + \gamma \rightarrow {}^{A-n}_{Z-n'} X^* + nN$$

$${}^{A-n}_{Z-n'} X^* \rightarrow {}^{A-n}_{Z-n'} X + \gamma$$

Irradiation by $8 - 30$ MeV photons

GRB 221009A

1. Brightest long GRB detected by the Swift Burst Alert Telescope (BAT) and Fermi Gamma-ray Burst Monitor (GBM) on October 9, 2022
2. Fermi Large Area Telescope (LAT) detected > 100 MeV γ rays in the 200-800 s time interval after the GBM trigger (T_0).
3. The highest-energy photon being of energy 99.3 GeV detected at $T_0 + 240$ s. This is the most energetic photon detected by Fermi-LAT from a GRB.
4. The burst isotropic-equivalent energy release $E_{\gamma,\text{iso}}$ is at least 3×10^{54} erg/s – among the highest measured

Emission models

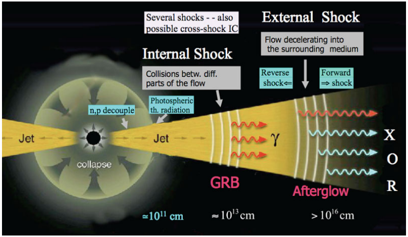

Figure: Schematic GRB jet from a collapsing star
(Image: Meszaros & Rees (https://ned.ipac.caltech.edu/))

- Internal shocks: most widely used model to interpret the prompt MeV emission
- External shocks: favored interpretation for long-term afterglows at high energies

Afterglow phases into gradually longer wavelengths over periods of days to months

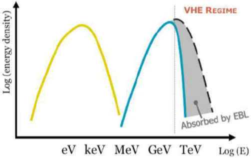

1. LE peak: Synchrotron emission of relativistic electrons
2. HE peak: Inverse-Compton scattering of synch photons

VHE ($\gtrsim$ 100 GeV) emission has been observed earlier from other GRBs during the afterglow decay phase (redshift, $z = 0.151$)

LHAASO observations

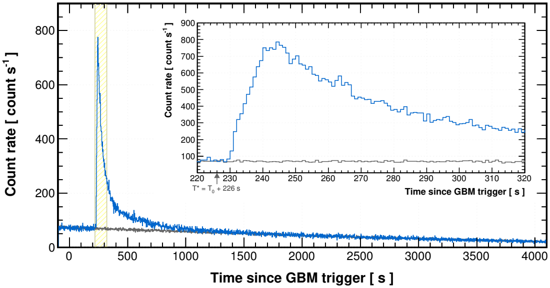

Figure: Count rate light curve of GRB 221009A observed by LHAASO-WCDA. Image: LHAASO collaboration (Science **380** (2023) 1390)

1. Within the first ~3000 s after the trigger, WCDA detected >64,000 photons with energies between ~200 GeV and ~7 TeV. Total LHAASO obs. time ~ 6000 s

LHAASO observations

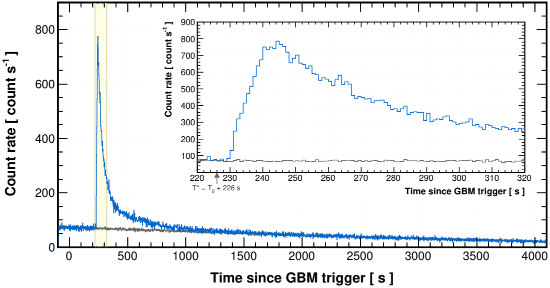

Figure: Count rate light curve of GRB 221009A observed by LHAASO-WCDA. Image: LHAASO collaboration (Science **380** (2023) 1390)

1. Within the first ~3000 s after the trigger, WCDA detected >64,000 photons with energies between ~200 GeV and ~7 TeV. Total LHAASO obs. time ~ 6000 s

2. The VHE emission exhibits a smooth temporal profile, with a rapid rise to a peak followed by a more gradual decay that persists for at least 3000 s after the peak.

Leptonic model (SYN+SSC)

- Fraction of shock energy in non-thermal electrons as $\epsilon_e = 10^{-2.5}\epsilon_{e,-2.5}$ and in turbulent magnetic field as $\epsilon_B = 10^{-4}\epsilon_{B,-4}$

- Electron distribution $dN/d\gamma \sim \gamma^{-1.74}$ and ISM particle density $n = 0.1 n_{-1}$ cm^{-3} – efficiency factor for electron acceleration to maximum energy E_c is $1/\phi = 0.1\phi_1^{-1}$

- We model the 0.1-1 GeV γ-ray flux using the SYN+SSC model, the break energies for time-dependent SYN spectrum are given as

$$\begin{aligned} E_m &= 28.6\,\epsilon_{e,-1.5}^{2}\epsilon_{B,-1.8}^{1/2}E_{55}^{1/2}t_{2.7}^{-3/2}\ \text{eV} \\ E_c &= 3.9\,\epsilon_{B,-1.8}^{-3/2}E_{55}^{-1/2}n_{-3.7}^{-1}t_{2.7}^{-1/2}\ \text{keV} \\ E_s &= 4.6\,\phi^{-1}E_{55}^{1/8}n_{-3.7}^{-1/8}t_{2.7}^{-3/8}\ \text{GeV}\,, \end{aligned} \tag{1}$$

at $t = 10^{2.7}t_{2.7}$ s post-trigger, when the blastwave is in a decelerating phase.

$$\rightarrow E^2\left(\frac{dN}{dE}\right) = 1.17\times10^{-6}\left(\frac{E}{\text{GeV}}\right)^{0.13}\ \text{erg cm}^{-2}\ \text{s}^{-1}; \qquad (E_c \le E < E_s)$$

Leptonic model (SYN+SSC)

Break energies in the SSC spectrum [Joshi & Razzaque (2021)]

$$E_{m,\mathrm{SSC}} = 1.5\, \epsilon_{e,-2.5}^{4} \epsilon_{B,-4}^{1/2} E_{55}^{3/4} n_{-1}^{-1/4} t_{2.7}^{-9/4}\ \mathrm{keV}$$
$$E_{c,\mathrm{SSC}} = 77\, \epsilon_{B,-4}^{-7/2} E_{55}^{-5/4} n_{-1}^{-9/4} t_{2.7}^{-1/4}\ \mathrm{TeV}\,. \quad (2)$$

$$\text{Klein} - \text{Nishina effect} \rightarrow E_{\mathrm{KN,SSC}} = 0.9\, \epsilon_{B,-4}^{3/2} E_{55}^{3/4} n_{-1}^{3/4} t_{2.7}^{-1/4}\ \mathrm{TeV}\,, \quad (3)$$

$$\textbf{SSC flux} \rightarrow E^2 \left(\frac{dN}{dE}\right) = 1.88 \times 10^{-7} \left(\frac{E}{\mathrm{GeV}}\right)^{0.63} \mathrm{erg\ cm^{-2}\ s^{-1}};\ (E_{m,\mathrm{SSC}} \leq E \leq E_{\mathrm{KN,SSC}})$$

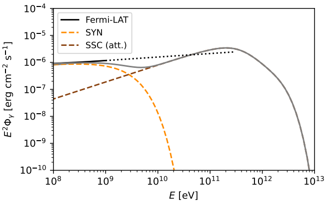

Figure: Estimated Fermi-LAT flux in the slow cooling regime (Das & Razzaque (2023) A&A)

EBL absorption

- SSC emission is sufficient to explain the published results by LHAASO for the flux spectra between 0.2 – 7 TeV.

- Photons of higher energy (if detected, and yet not published by LHAASO), EBL absorption becomes important for intrinsic emission.

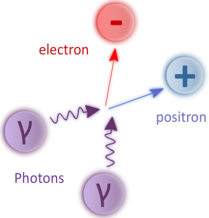

$$\gamma + \gamma_{\rm bg} \rightarrow e^+ + e^-$$ *Breit-Wheeler Process*

HE γ-rays collides with EBL photons

Annihilated by e^+e^- pair production

$$\epsilon_\gamma \epsilon_{\rm bg} \geqslant = \frac{2m_e^2c^4}{\epsilon_\gamma(1-\cos\theta)}$$

$\Longrightarrow$ Lorentz Invariance Violation/ Mixing with axion-like particles.

UHECR interactions

- For emission at energies higher than > 3 TeV, simple synchrotron and synchrotron self-Compton model is not sufficient

- Klein-Nishina effect leads to a spectral steepening in the SSC emission

- Reverse shock proton synchrotron emission [Zhang et al. (2023)]
- Lorentz Invariance Violation [Finke & Razzaque (2023), Baktash et al. (2022), Li & Ma (2022)]
- Mixing with axion-like particles [Galanti et al. (2022), Baktash et al. (2022), Troitsky (2022)]

γ-ray bursts are also a potential candidate class of
UHE cosmic-ray ($E \gtrsim 10^{17}$ eV) acceleration

- UHECRs undergo a variety of interactions with CMB and EBL photons during their propagation – secondary $e^{\pm}$, γ rays - initiate electromagnetic cascade

UHECR propagation

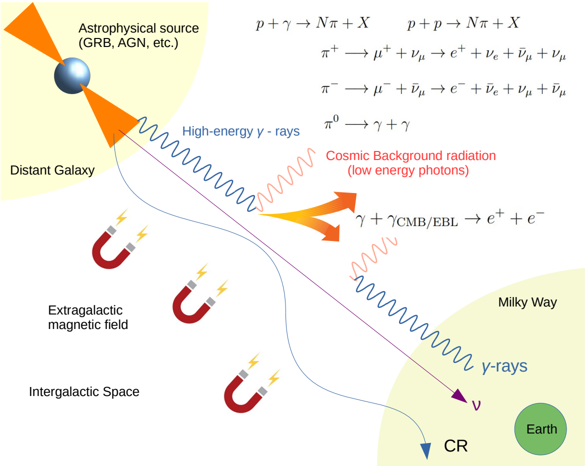

Figure: Ultrahigh-energy cosmic ray propagation over cosmological distances. (Figure created using Libre Office Draw)

Lepto-hadronic model

UHECR acceleration in the external shock
of the GRB blastwave, during the afterglow emission phase

- Maxm. proton energy for adiabatic blastwave in a constant density environment [Razzaque (2013)] $E = 9.7 \times 10^{19} \phi^{-1} \epsilon_{B,-1.8}^{1/2} E_{55}^{3/8} n_{-3.7}^{1/8} t_{2.7}^{-1/8}$ eV

1. EM cascade initiated by secondary e$^{\pm}$ can produce secondary γ-ray spectrum that peaks at ~ 1 TeV energies, and extends down to GeV energies.

- EGMF deflects the UHECRs from our line of sight – resultant flux can be a fraction of the emitted flux

- The time delay induced by deflection in the EGMF can be expressed as

$$\Delta t_{\rm IGM} \approx \frac{d_c^3}{24 r_L^2 c N_{\rm inv}^{3/2}} \approx 2000 \text{ s} \left(\frac{d_c}{648 \text{ Mpc}}\right)^{3/2} \times \left(\frac{\lambda_c}{1 \text{ Mpc}}\right)^{3/2} \left(\frac{B}{1.82 \times 10^{-5} \text{ nG}}\right)^2 \left(\frac{E}{100 \text{ EeV}}\right)^2$$

Cosmogenic γ rays

- CRPropa3.2 – UHECR propagation [Alves Batista et al. 2022, 2023]

- We consider a proton spectrum of the form $dN/dE_p \sim E^{-2}$ in the energy range 0.1-100 EeV, and a random turbulent EGMF, given by a Kolmogorov power spectrum.

- RMS magnetic field strength of $B_{\rm rms} \approx 1.82 \times 10^{-5}$ nG, and a coherence length of $\lambda_c \sim 1$ Mpc, so that $\Delta t \simeq 2000$s – consistent with LHAASO observation time

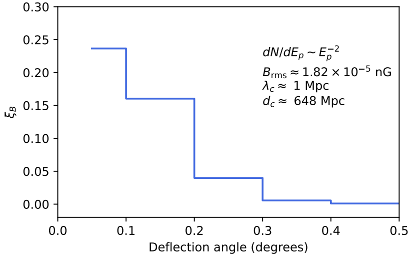

Figure: Fraction of UHECRs that survives within $0^\circ.1$ of the initial emission direction (Das & Razzaque (2023) A&A)

LHAASO $\gtrsim 10$ TeV photons

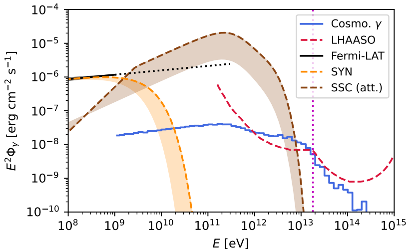

Figure: Line of sight cosmogenic γ rays from UHECR interactions (Das & Razzaque (2023) A&A)

- Upper bound: $\epsilon_e = 10^{-1.5}\epsilon_{e,-1.5}$, $\epsilon_B = 10^{-1.8}\epsilon_{B,-1.8}$ – Lower bound: $\epsilon_e = 10^{-2.5}\epsilon_{e,-2.5}$ and $\epsilon_B = 10^{-4}\epsilon_{B,-4}$

- UHECR luminosity in the energy range from 0.1-100 EeV

$$L_{\mathrm{UHE}p} \gtrsim \frac{2\pi d_L^2(1-\cos\theta_j)}{\xi_B f_{\gamma,p}} \int_{1\,\mathrm{GeV}}^{100\,\mathrm{EeV}} \epsilon_\gamma \frac{dn}{d\epsilon_\gamma dAdt} d\epsilon_\gamma$$

Neutrinos from GRB

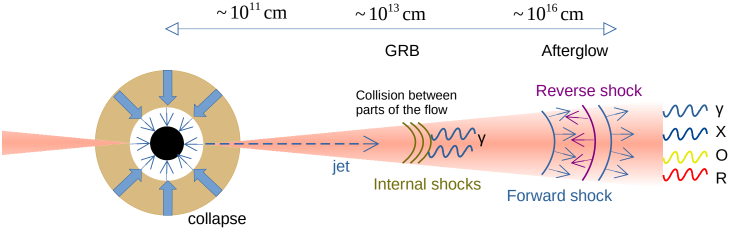

Figure: In long GRBs, the core collapse of a massive star launches a relativistic jet that propagates through the dense stellar envelope. (Figure created using Libre Office Draw)

- $p\gamma$ interactions in the internal shocks – PeV neutrinos and external shocks – EeV neutrinos.
- Before jet breaks out of the progenitor – $p\gamma$ interaction with thermally trapped X-ray photons – TeV neutrinos
- pp interaction in baryon-dominated dissipative photosphere – PeV neutrinos and suppress PeV component due to rapid cooling of protons
- Neutron rich ejecta, p and n decouple casting with different Lorentz factors – relative speed > 145 MeV – collisions – multi-GeV neutrinos

Cosmogenic neutrinos

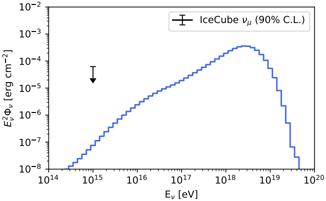

Figure: Cosmogenic neutrino fluence, from UHECR propagation, in 2 hrs of IceCube operation

- UHECRs accelerated in internal shocks – $p\gamma$ with prompt γ-rays – PeV neutrino production – IceCube non-detection within 3 hrs of Fermi-GBM trigger

- Time integrated upper limit in 0.8-1 PeV energy range – implications for GRB model parameters (Murase et al. 2022, Ai & Gao 2022, Liu et al. 2023)

- $p\gamma$ interaction with afterglow photons – neutrinos in the EeV range – hence IceCube limits are not applicable

Summary I

- beaming corrected luminosity $L_{\mathrm{UHE}p} \gtrsim 5.4 \times 10^{47}$ erg/s – isotropic equivalent energy release of $\gtrsim 3.9 \times 10^{53}$ ergs.
- SSC spectrum falls off sharply beyond ~ 220 GeV. However, the SSC spectrum is consistent with Fermi-LAT observation of ~ 100 GeV photon.
- Additional time delay due to propagation in the host galaxy (Takami & Murase 2012). which for GRB 221009A at $z < 1$ can be a compact galaxy (Schneider et al. 2012) – unknown B
- For our model to be valid, the GRB needs to be positioned at the outskirts of the host galaxy or away from the disk region, so that the magnetic field is diminished.